Non-Destructive Testing of Steel Wire Rope Using Magnetic Flux Leakage: Principle, Sensor Design and Signal Wavelet Analysis

Xiaoyong Zhong, Xiaohong Zhang

School of Science, Jiangxi University of Science and Technology, Ganzhou Jiangxi, China
E-mail: zhongxy52@163.com

Abstract **- As a kind of flexibility bearing component, steel wire ropes are applied widely. However, after being used for a period, some flaws may be produced in the steel wire rope. In order to ensure the safe operation of steel wire ropes, non-destructive testing methods are being applied to inspect steel wire ropes. In this paper, an intelligent non-destructive testing equipment, consisting of the sensing detectors and signal analysis computer system, has been designed and constructed. Any geometrical discontinuity in magnetic permeability in the magnetized steel wire rope will cause the magnetic field to leak out of the rope. The flux leakage fields which conceive information on anomalies, such as broken wires, abrasion, corrosions, are measured by Hall sensor array. However, these signals contain a lot of noises which make the flaws difficult to analyse. In this paper, the implementation of a wavelet transform has been used to characterize and analyse signals of the wire rope flaws obtained from the non-destructive testing equipment. Related experiments are performed based on the equipment. Repeatability, resolution and sensitivity of the signals are also assessed to show the performances of the instrument.**

Keywords - steel wire rope; non-destructive testing; magnetic flux leakage; wavelet transform; Hall sensor array

I. INTRODUCTION

Steel wire ropes are widely used in metallurgical industry, mining, transport, building, tourism, cable-strayed bridges, architecture, etc. However, after being used for a period, some flaws may be produced in the steel wire rope. Deteriorations of the steel wire rope, such as broken wires, corrosion, fatigue, abrasion or wear cause the declination of the structure strength of the steel wire rope[1-3]. And they maybe even lead to catastrophes. The safe operation of wire rope receives more and more attention nowadays.

The studied methods of inspection contain acoustic emission, electromagnetic method, X-ray and others, among them, electromagnetic method is practical and robust [4-7]. The main technologies applied in the non-destructive testing of ferromagnetic ropes are based on the magnetic inspection (MI) and in particular on the magnetic flux leakage (MFL) and the magnetic reluctance variation (MRV) techniques [8-11]. Before the steel wire rope faults are tested, the magnetizer must magnetize the test material to saturation. Then, any geometrical discontinuity and local gradients in magnetic permeability in the test object will cause the magnetic field to leak out of the object and into the air. The magnetic leakage flux conceives information on inclusions or anomalies, such as broken wires, abrasion, corrosions is measured by a magnetic field sensor, and the dimensions or positions of the defects can be realized by the proper digital information processor. Some steel wire rope detectors attain one sensor, another use many sensors.

The measurement of the magnetic field is usually provided by two main sensor technologies: coils and Hall sensors. The first kind of sensor is very sensitive to local flux variation produced by defects. Its signal amplitude is related to the scanning velocity. As a result of the limitation of volume, to get high flaw resolution with coil sensor is very difficult. On the contrary, Hall sensors allow the measurement of the absolute value of the magnetic flux density (B). Because Hall sensor dimension is very small, the resolution of instrument with Hall sensor could be higher, and by using array of them, new concept sensor topologies can be developed [12-13]. Many aspects influence equipment’s resolution and reliability: detector topology, magnetic saturation level of the body under test, sensor technologies, position and dimension of the defects, signal process methods, etc[14].

In this paper, an innovative testing equipment using Hall sensor to measure magnetic flux leakage for evaluating the deterioration of steel wire ropes is designed and constructed. The testing equipment consists of the sensing detectors and signal analysis computer system. In most case, the flaws are not easy to analyze[15], because there are many noises contained in the inspection signal ,which caused by electronic components, complex spiral structure of the wire rope itself and variation due to the gap between the steel wire rope and the testing detector. Especially, when the dimension of flaw is small and the broken wire is in the interior of the steel wire rope, the leakage magnetic field and sensor electric potential are weak, there is no evident signal of flaws in the testing signals wave. Suitable signal processing techniques are needed to analyze the MFL signal characters. Wavelet analysis researches the character of signal by detecting all changes under different scales which makes it adapt to analyse some aberrant signals caused by defeats in steel wire rope [15-16].

II. PRINCIPLE OF NON-DESTRUCTIVE TESTING

A. Leakage Magnetic Field

In magnetic flux leakage testing of wire rope, the leakage magnetic field is a constant magnetic field. According to the Maxwell's equations, the constant magnetic field will meet following equations:

$$\begin{cases} \oiint_s B \cdot dS = 0 \\ \oint_l H \cdot dl = \sum I_0 \end{cases} \quad (1)$$

where B is the magnetic field density, is the magnetic field intensity and is the conduction current.
The equations (1) is applied to two magnetic media interfaces, as shown in Fig. 1.

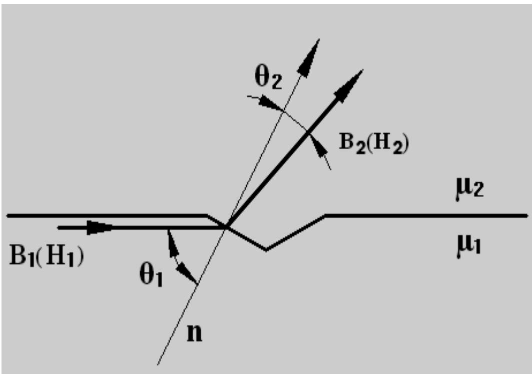

Fig. 1 Refraction of magnetic field lines on different media

Where n is unit normal vector, B_1 and H_1 are the magnetic field density and the magnetic field intensity of medium 1 respectively. B_2 and H_2 are the magnetic field density and the magnetic field intensity of medium 2 respectively. Θ_1 is the angle between magnetic field lines on the medium 1 and the normal n. Θ_2 is the angle between magnetic field lines on the medium 2 and the normal *n*.

Because the conduction current is zero on the interface of different media, from the equations (1) the following equations can be concluded:

$$\begin{cases} n \cdot (B_2 - B_1) = 0 \\ n \times (H_2 - H_1) = 0 \end{cases} \quad (2)$$

Equations (2) can be expressed as:

$$\begin{cases} B_1 \cos\theta_1 = B_2 \cos\theta_2 \\ H_1 \sin\theta_1 = H_2 \sin\theta_2 \end{cases} \quad (3)$$

In the isotropic homogeneous magnetic medium: $B_1 = \mu_1 \mu_0 H_1$, $B_2 = \mu_2 \mu_0 H_2$. Where μ_1 is relative magnetic permeability of medium 1, is relative magnetic permeability of medium 2.

From equation (3), equation (4) can be concluded:

$$\frac{\tan\theta_1}{\tan\theta_2} = \frac{\mu_1}{\mu_2} \quad (4)$$

The permeability of the ferromagnetic material is greater than that of non-ferrous magnetic material, for example, air. If there is no defect in the magnetized rope, magnetic field lines pass through the rope uniformly, as shown in Fig. 2(a). When there is defect in the magnetized rope, part of the magnetic field lines refract into the air, through the air to the other side of the defects, as shown in Fig. 2(b).

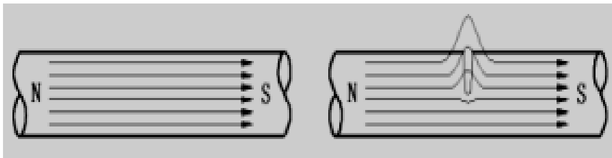

(a) Intact condition (b) Damaged condition
Fig. 2 Magnetic field lines in steel wire rope

According to the flaw features of the steel wire rope, the flaw is simplified to slot, and the defect field, the leakage field is shown in Fig. 3. From Fig. 3, it can be known that tangential component of magnetic flux leakage is bilateral symmetric, and normal component of magnetic flux leakage is central symmetric. In Fig. 3(a), the maximum amplitude point is corresponding to the place of the maximum flaw. In Fig. 3 (b), two extreme points of normal component correspond to the two cross-sections of the flaw, and zero point is the place of the maximum flaw. And the value of the magnetic leakage flux is related with the defect's extent.

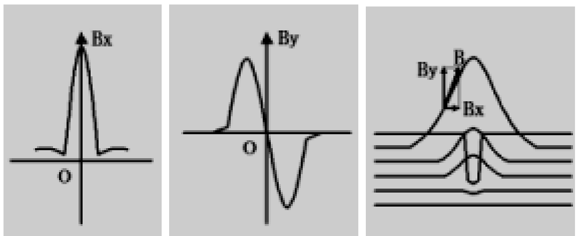

(a) Tangential component (b) Normal component (c) Magnetic flux
Fig. 3 Diagram of magnetic flux leakage field with flaw

-B. Magnetic Flux Leakage Testing Model

If there is any flaw in the magnetized wire rope, and then there is a leakage magnetic field near the flaw. The magnetic flux leakage can be divided into three parts, as shown in Fig. 4. The first part (indicated 1) is insensitive to flaw, always existing around the magnetized wire rope, named the stray magnetic flux leakage; the second part (indicated 2) is closely related to defect, known as the flaw diffusion of magnetic flux leakage; the third part (indicated 3), the magnetic field lines direct through fractures, is known as a broken internal magnetic flux leakage. It is clear that only the flaw diffusion of magnetic flux leakage part is easy to measure.

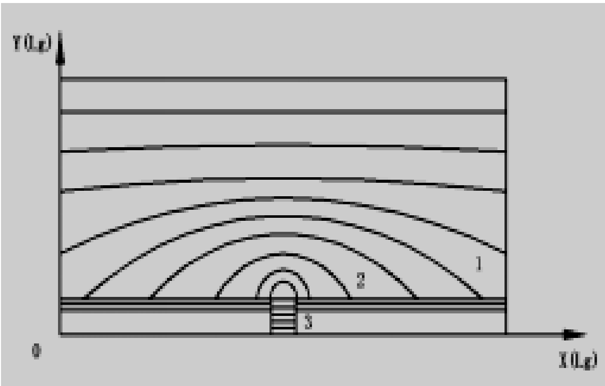

Fig. 4. Leakage magnetic field distribution

The defect can be simplified to rectangular slot. In order to facilitate the calculation, the origin of X, Y coordinates adjust to the defect location, as shown in Fig. 5.

The magnetic intensity in the slot is placed evenly. The magnetic intensity is in inverse proportion to the distance away from the defect. Leakage flux above the defect can be given below:

$$\begin{cases} H_x = \left(\frac{H_g L_g}{\pi}\right)\left(\frac{y}{x^2+y^2}\right) \\ H_y = \left(\frac{H_g L_g}{\pi}\right)\left(\frac{x}{x^2+y^2}\right) \end{cases} \quad (5)$$

where is the magnetic intensity in the slot, is width of the slot. If , the value of leakage flux can be expressed as:

$$\begin{cases} H_x(x=0) = \frac{H_g L_g}{\pi y} \\ \left(\frac{dH_y}{dx}\right)_{x=0} = \frac{H_g L_g}{\pi y^2} \end{cases} \quad (6)$$

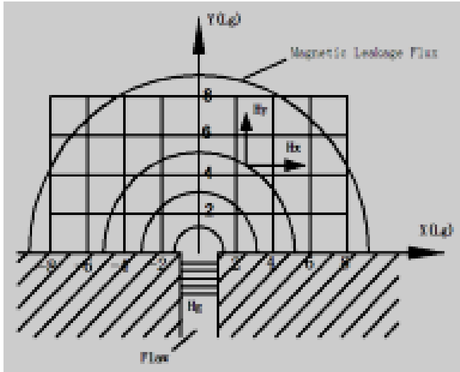

Fig. 5. Sketch map of Foster theory

From Equ. (6), the value of leakage flux is in direct proportion to H_g L_g and in inverse proportion to y. The sensitivity of leakage flux to sensor is in direct proportion to H_g L_g and in inverse proportion to y^{-2} .Thus, when the value of L_g remains invariant, the magnetic intensity H_g becomes stronger, the leakage flux will become larger, and the sensitivity of leakage flux will also become more sensitive.

III. DESIGN OF THE NON-DESTRUCTIVE TESTING SYSTEM

A. Configuration

The diagram of the non-destructive testing system of wire rope designed in the paper is shown in Fig. 6. In the process of detecting, the wire rope makes relative movement with the sensing detector. The magnetic field signal around the wire rope is picked up by magnetic sensors, and then is magnified and demodulated in signal pre-processor. After pre-processed, the detecting signal is converted by A/D converter to digital signal which can be identified and processed by the computer.

The digital signal is input into the computer through I/O interface. Then it can be disposed by many signal processing methods, such as wavelet transform, and the aim is to filter the interference signals and enhance the signal to noise ratio.

At last, the final testing results are outputted through display and printer. In order to obtain the defect position, a displacement sensor is set on the sensing detector, and the displacement signal is also transferred into the computer. The displacement signal and defect magnetic field signal are simultaneously processed, the defect state of every place of the whole wire rope can be obtained, and then the quantitative detection of the steel wire rope can be realized.

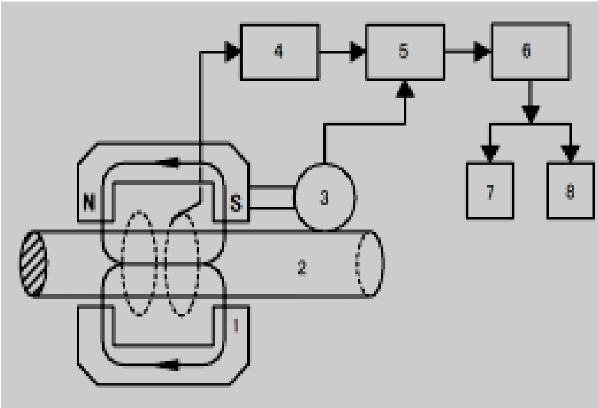

1- sensing detector; 2- wire rope; 3- isometry pulse generator;4- signal pre-processor;
5- A/D converter; 6-computer; 7-disply; 8-printer
Fig. 6. Configuration of non-destructive testing system of wire rope

B. Magnetization Curve

To magnetize steel wire rope, there are three exciting methods, that is, DC excitation, AC excitation and permanent magnet excitation. There is skin effect in wire rope with AC excitation, thus measurement accuracy in this way is not high. Compare to the DC power source for steel wire rope magnetization, the permanent magnet excitation for the steel wire rope magnetization is simple, reliable, low-cost[17]. So the paper adopts permanent magnet excitation method.

A 6×19, Φ24mm wire rope magnetization characteristic curve is shown in Fig. 7. In order to obtain the best effect of magnetization while magnetic flux leakage inspection, wire rope magnetization should be chosen the right of M point on the deep saturated zone. In this way, leakage of magnetic flux to wire rope defects would be more obvious, so as to increasing the sensitivity of magnetic flux leakage test.

C. Equivalent Magnetic Circuit

The sensing detector is composed of excitation magnetizers and sensors, and they are key components of signal processing and flaw test. Equivalent magnetic circuit model is shown as in Fig. 8. Where, is equivalent magnetic resistance of wire rope, is equivalent magnetic resistance of gap between permanent magnet and the wire rope, is magnetic resistance of the permanent magnet, is magnetic resistance of armature iron, is equivalent magnetic resistance of the permanent magnet flux leakage, F_m is the magneto-motive force of permanent magnets(usually rare earth permanent magnet NdFeB). Φ_r ,Φ_t , Φ_a , are magnetic flux of loops respectively. When rare earth permanent magnet magnetic energy product is bigger, and the magnetic resistance of excitation circuit is appropriate, permanent magnet flux Φ_m is approximate to constant.

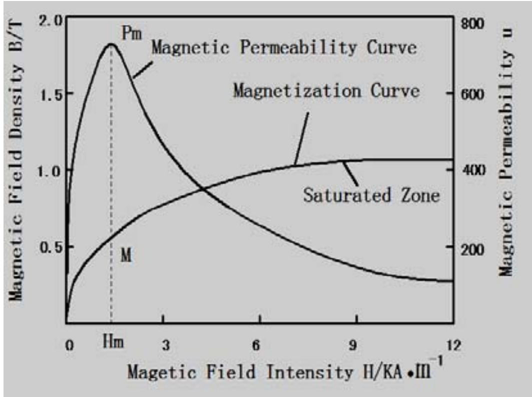

Fig. 7. The magnetizing curve of 6×19, Φ24mm wire rope

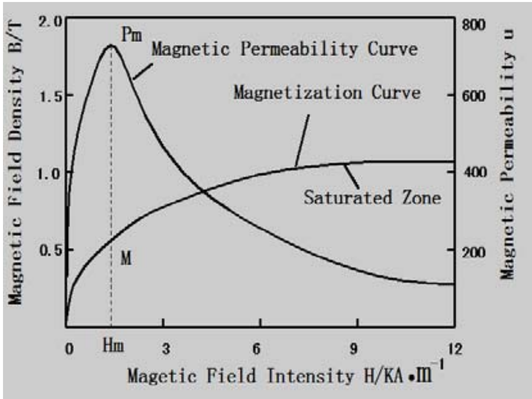

Fig. 8. The equivalent magnetic circuit model

In Fig. 8 for A:

$$\phi_m = \phi_a + \phi_t \qquad (7)$$

For B:

$$\phi_m = \phi_r + \phi_t \qquad (8)$$

For loop1:

$$\phi_r(2R_g + R_r) + \phi_m R_m + \phi_a R_a + \phi_m R_m = 2F_m \qquad (9)$$

For loop2:

$$\phi_t R_t + \phi_m R_m = F_m \qquad (10)$$

From equations 7 to 10, magnetic flux through wire rope can be expressed as:

$$\phi_r = \frac{2R_t}{2R_g + R_r + R_a + 2R_t}\phi_m \qquad (11)$$

and

$$B_r = \frac{\phi_r}{S_r} \qquad (12)$$

where B_r is the magnetic field density of the tested wire rope, S_r denotes its equivalent cross-sectional area.

Wire rope non-destructive testing excitation structure is established according to the characters of wire rope defect. The value of magnetization intensity is determined by the influence of magnetization intensity to localized fault (LF) and loss of metallic cross-sectional area (LMA) defection signals. Meanwhile, whether the rope can be magnetized to saturation is regarded as a standard for a rational design. Based on the equivalent magnetic circuit of excitation structure, parameters of excitation structure size are obtained, and then an analysis is made of the impacts of the excitation structure size variation to excitation. A value of intensity could be achieved by adjusting the key dimension values, and the last dimension values provide a reference for the excitation structure dimension design.

D. Sensor

The detection of the magnetic field is usually provided by two main sensor technologies: coils and Hall sensors. The behaviors of coil sensors are based on Faraday law and so give a signal proportional to the flux variation. The amplitude of signal of coil sensors is related to the scanning velocity. As a result of the limitation of volume, it is very difficult to get high flaw resolution with coil sensor. On the contrary, Hall sensors allow the measurement of the absolute value of the magnetic flux density, as shown in Fig. 9.

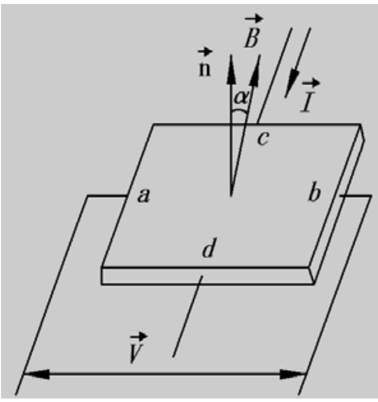

Fig. 9. Working principle of Hall sensor

The output voltage of Hall element can be expressed as:

$$\vec{V} = K(\vec{B} \times \vec{I}) \qquad (13)$$

In the equation (13), is the sensitivity coefficient of the Hall element and is constant in certain conditions, which is affected by the size, material of Hall element, working temperature. Electric current pass through the two sides of Hall element. When the steel rope to be tested has been magnetized, leakage magnetic field B will generate Hall potential V. From equation (13), Output voltage of Hall sensor is no relevant with the scanning velocity

On the other hand, as Hall sensor dimension is very small, the resolution of instrument with Hall sensor could be higher, but the detection range of individual Hall sensor is relatively small. And new concept sensor topologies can be developed by using Hall element array. In the paper, a Hall element array arranged uniformly around the wire rope is proposed, as illustrated in Fig. 10, with which axial and circumferential flux leakage information around wire rope can be obtained.

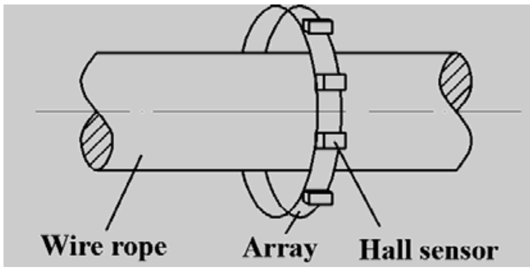

Fig. 10. Array of Hall sensors

The number of Hall sensors is:

$$N \geq \frac{360^{\circ}}{\theta} \qquad (14)$$

Where is a Hall sensor's testing scope, as shown in Fig. 11. When a flaw of wire rope is in testing scope of a Hall sensor, the flaw can be inspected by the Hall sensor.

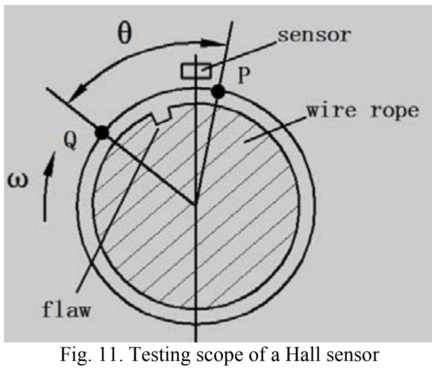

Fig. 11. Testing scope of a Hall sensor

E. Detector

In the structure design of detector, NdFeB permanent magnets surround the tested wire rope, and its magnetization is along the length direction of the wire rope. In order to obtain the MFL signal of the defects accurately and reliably, the three restrictions should be taken into consideration. Firstly, the magnetic field density must be strong enough to measure the amount of the magnetic flux leakage from the flaws. Secondly the detecting head's diameter adapts to the tested wire rope's

DOI 10.5013/IJSSST.a.17.26.26 ISSN: 1473-804x online, 1473-8031 print

diameter and changes with it, the detecting head should be replaced easily. Lastly a length of space should be created in the middle of the two permanent magnets for placing the sensor arrays.

There is a certain gap between the wire rope and the sensor. The gap depends on the defect magnetic leakage field value, the detecting space and sensitivity of the Hall sensor. In addition a proper gap can reduce the attractive power of the sensor to the rope, and make the rope move conveniently when testing. Therefore, a wire rope detector may be consists of a set of magnetic alternative heads, with which the detector can detect flaws of different diameter wire ropes sensitively. The weight, dimension and configuration of detectors are primarily divided into three types. The parameters of detectors are shown in table 1. All the presented sensing detectors have been designed by using 3D magnetic simulations performed by the FIT technique. The views of sensing detectors are shown as Fig. 12.

The magnetic signal detected by the sensing detectors can be used to analyze the flaws sometimes. As the noises are still contained in the original inspection signal, in most case the flaws are difficult to analyze. Especially when the dimension of flaw is small, and the broken wire is in the interior of the steel rope, and the leakage magnetic field and sensor electric potential are weak, there is no evident signal of flaws in the testing signals wave.

TABLE 1 SENSING DETECTOR SPECIFICATION PARAMETERS

Sensing Detector	Dimensions Weight	Wire Rope Diameter	Alternative Heads	Scanning Velocity Range
detector 1	90×150×300mm 4kg	16-19mm	FixedΦ16-19mm	0.3-3m/s
detector 2	90×195×300mm 8kg	20-49 mm	Φ20-24mm; Φ25-29mm; Φ30-34mm Φ35-39mm; Φ40-44mm; Φ45-49mm	0.3-3m/s
detector 3	190×280×300mm 12kg	50-64 mm	Φ50-54mm; Φ55-59mm; Φ60-64mm	0.3-3m/s

(a) detector 1 (b) detector 2 (c) detector 3

Fig. 12 The profile of sensing detector

Several signal processing techniques are implemented to de-noise and analyze the MFL inspection signals. The wavelet analysis has excellent and local nature in time and frequency field, and valuable information can be acquired from disturbed signals. The MFL signal can be divided into respective component of different frequency and time fields. The wavelet transform implementation is then used to analyse the inspection signal in this paper.

IV. EXPERIMENT RESULTS AND DISCUSSION

In the experiments, a 6×19 steel wire rope is selected, its diameter being 24mm, which consists of 6 strands, each strand comprises of 19 individual wires. The 6 strands are manufactured in left ray. Artificial defects are made to the rope for testing as illustrated in Fig. 13. In the figure, A, B, C and D are defects with a constant width of 2 mm and a distance of 40 mm apart from each other. Their depths are 1.5, 2.5, 3.5 and 4.5mm respectively, representing the variation of depth of defects. E and F have a 2.5 mm constant depth and a width of 3 and 5 mm respectively. They exist a 20mm interval for testing the resolution of the instrument. G is a group of 3 defects, H is the smallest defect with 1mm width and 1 mm depth, for testing the sensitivity of the instrument. I and J are subsurface defects. These two 4mm wide defects are located at 3mm under the surface.

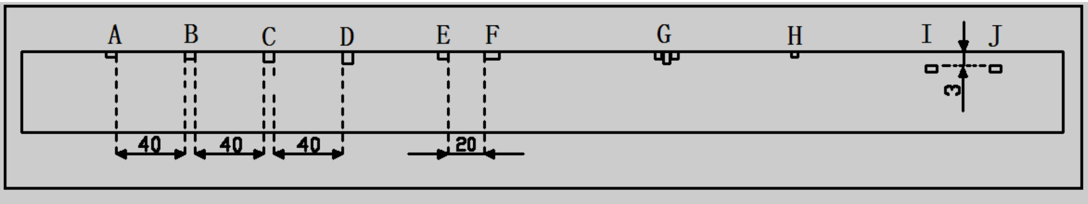

Fig. 13. Diagram of location of artificial defects

The signal received from the detecting element oscillates with different amplitude and duration time. It consists of various frequency components. The consequence of inspection signal waveform is showed in Fig. 14.

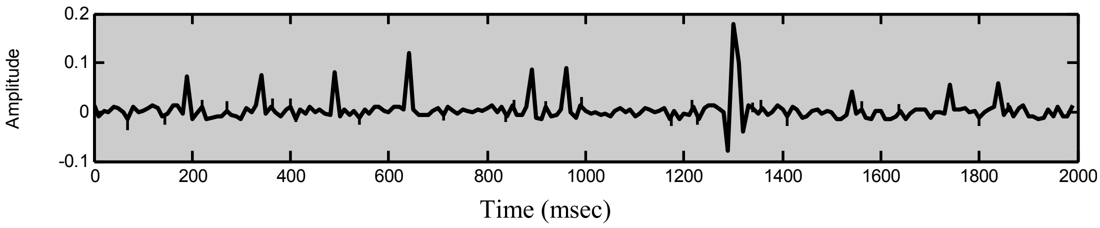

Fig. 14. Inspection magnetic signal waveform of wire rope

To de-noise the MFL inspection signal, the frequency ingredients of the signal are decomposed by using wavelet transform. The processing steps are given below:

(1) Select proper wavelet function, all these inspection signals are decomposed into various frequency bands using wavelet analysis.

(2) Some trashy signals must be filtered in order to filter and reshape the MFL inspection signals.

MFL signals are transient signals in different amplitudes and duration times, the Daubechies (db) family which is orthogonal, compact and nearly symmetrical can be applied in this case. So the MFL signals are analysed by using the 'db4' function in the wavelet transform. The wavelet function and scale function of 'db4' are shown in Fig. 15.

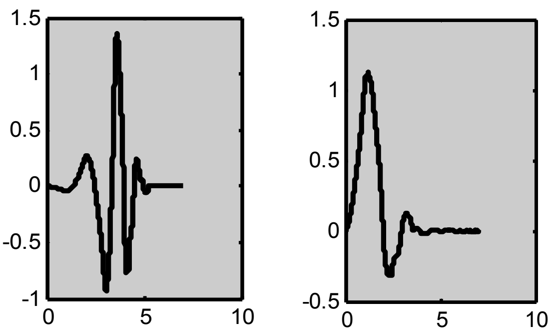

(a) wavelet function (b) scale function

Fig. 15. The wavelet function and scale function of 'db4'

The decomposition process is able to iterate in multi-level of resolution components. Because the low frequency ingredient is main component of the MFL signal in the paper, the discrete wavelet transform is implemented for analyzing. The suitable level of decomposition is based on a suitable criterion and the character of the signal. The inspection signal received from the Hall elements contains high frequency noises, but the amplitude of the high frequency noises is not too high. So, 3 levels of the wavelet decomposition tree are suitable for de-noising the inspection signal. The 3 levels of wavelet decomposition tree for de-noising the inspection signal is illustrated in Fig. 16.

In Fig. 16, the decomposition analysis in 3 levels has been implemented to de-noise the MFL signal, where the decomposed signal can be expressed as:

$$S = A3 + D3 + D2 + D1 \qquad (15)$$

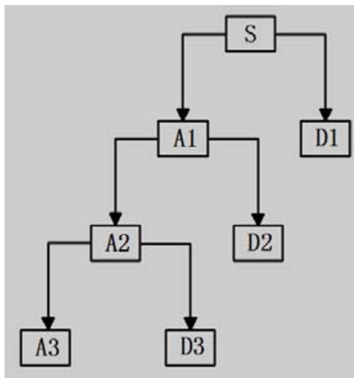

Fig. 16 The 3 levels wavelet decomposition tree

Using the wavelet transform, the inspection signal can be decomposed into different frequency elements. In this way, according to the feature of noise and the useful defect signals, wavelet coefficient can be chosen, then rebuild the signal according to the coefficient that has been dealt with. So the filtered signal of wavelet can be acquired in frequency. Fig. 17 displays the inspection signal waveforms which are reconstructed by using DWT.

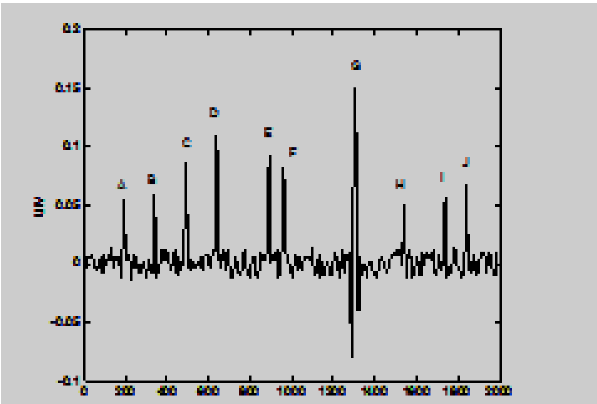

Time (ms)

Fig. 17. Reconstructed inspection signal using DWT

In Fig. 17, the inspection signal is decomposed and reconstructed in 3 levels which have good revelations to the defects of the wire rope. The signal amplitude can identify the defect items E and F. From the result, it can be seen that the instrument can be used to classify two defects which are located 20 mm from each other, with better spatial resolution than 20 mm. Meanwhile the result shows that the instrument is able to detect the smallest defect H peak amplitude, with high sensitivity at depth and width 1mm respectively.

V. CONCLUSION

In this paper, a magnetic flux leakage instrument has been designed and developed to detect the flaws of steel wire rope. The instrument is composed of a variety of series of sensing detectors suitable for different diameter wire ropes and signal analysis computer system. The axial and circumferential flux leakage fields around wire rope are measured by Hall sensor array. To extract value signal from the inspection signals containing various noises, the wavelet transform theory is applied to the resolution and reconstruction of the inspection signals. Related experiments are performed based on the equipment. Various types (depths and widths, locations) of defects are employed to investigate the performance of the equipment. Results show that the equipment can be employed to inspect defects of wire rope and represent performances of good resolution, repeatability and sensitivity.

ACKNOWLEDGMENT

This work was supported by the National Natural Science Foundation of China (Grant Nos: 11062002, 61363076), and the Key Science and Technology Project of Jiangxi Provincial Department of Education (Grant Nos: GJJ14439, GJJ14465), the National Natural Science Foundation of Jiangxi Province (Grant No: 2014BAB207020).

REFERENCES

[1] Alexander Vorontsov, Alexander Zhirnov, Dmitry Sukhorukov. Magnetic NDT and computer modeling of steel ropes deterioration in suspended bridges[J]. Key Engineering Materials, 2013, 31(569-570): 1101-1108.

[2] Bertrand Fernandes, Michael Titus, Douglas Karl Nims, et al. Practical assessment of magnetic methods for corrosion detection in an adjacent precast, prestressed concrete box-beam bridge[J]. Nondestructive Testing and Evaluation, 2013, 28(2): 99-118.

[3] K. Schrems and D. Maclaren. Failure analysis of a mine hoist rope[J]. Eng. Failure Anal., 1997, 4(1): 25-38.

[4] Weischedel H R. The Inspection of Wire Ropes in Service[J]. Wire Journal International, 1985, 9: 180-198.

[5] Kalwa E, Piekarski K. Detection of Defects in a Steel Rope with the Hall-Effect Magnetic Probe.C.S[J]. NDT Journal, 1987, 8(2): 46-49.

[6] Yanhua Sun, Jianbo Wu, Bo Feng, and Yihua Kang. An Opening Electric-MFL Detector for the NDT of In-Service Mine Hoist Wire[J]. IEEE Sensors Journal, 2014, 14(6): 2042-2047.

[7] M. Goktepe. Non-destructive crack detection by capturing local flux leakage field[J]. Sens. Actuators A, Phys., 2001, 91(1): 70-72.

[8] F. Forster. New findings in the field of non-destructive magnetic leakage field inspection[J]. NDT Int., 1986, 19(1): 3-14.

[9] Sanjay Kumar & Dalgobind Mahto. Recent Trends in Industrial and other Engineering Applications of Non Destructive Testing: A Review[J]. Global Journal of Researches in Engineering General Engineering, 2013, 13(3): 29-46.

[10] Mukhopadhyay, S., Srivastava, G.P.: Characterisation of metal loss defects from magnetic flux leakage signals with discrete wavelet transform[J]. NDT E Int., 2000, 33(1): 57-65.

[11] Seunghee Park, Ju-Won Kim, Changgil Lee, et al. Magnetic Flux Leakage Sensing-Based Steel Cable NDE Technique[J]. Shock and Vibration, 2014(2014): 1-8.

[12] Cao, Y., Zhang, D., Wang, C., et al.: More accurate localized wire rope testing based on Hall sensor array[J]. Mater. Eval, 2006, 64(9): 907-910.

[13] SushantM Dutta, FathlH Ghorbe and RoderieK Stanley. Simulationandanalysis of 3-D magnetie fluxleakage[J]. IEEE Transon MAGN., 2009, 45(4): 1966-1972.

[14] Renaldas Raišutis, Rymantas Kažys, Liudas Mažeika, et al. Ultrasonic guided wave-based testing technique for inspection of multi-wire rope structures[J]. NDT&E International, 2014, 62: 40-49.

[15] C. Jomdecha, A. Prateepasen and W.Methong. Characterization of Wire Rope Defects from Magnetic Flux Leakage Signals[J]. Thammasat International Journal of Science and Technology, 2003, 8(1): 54-63.

[16] F. Truchetet, O. Laligant. Wavelet Applications in Industrial Processing II[J]. Proc. of SPIE Vol. 5607, 2004: 1-14.

[17] Xiaoyong Zhong, Xiaohong Zhang. Research of Non-destructive Testing of Wire Rope Using Magnetic Flux Leakage[J]. Applied Mechanics and Materials, 2012, 189: 255-259.